engineering proceedings

MDPI

Proceeding Paper

Sensorless Speed Control of Induction Motor Using Model Reference Adaptive System and Deadbeat Regulator †

Wail Hamdi [1,*], Mohamed Yacine Hammoudi [1] and Achour Betka [2]

[1] Laboratory of Energy Systems Modeling (LMSE), Department of Electrical Engineering, University of Biskra, Biskra 07000, Algeria
[2] Laboratory of Electrical Engineering of Biskra (LGEB), Department of Electrical Engineering, University of Biskra, Biskra 07000, Algeria
* Correspondence: wail.hamdi@univ-biskra.dz
† Presented at the 4th International Electronic Conference on Applied Sciences, 27 October–10 November 2023; Available online: https://asec2023.sciforum.net/.

Abstract: This paper presents the sensorless speed control of induction motors using a Model Reference Adaptive System (MRAS) method and field-oriented control. The main objective is to minimize the cost related to speed sensors, thereby improving both the affordability and efficiency of motor control. The sensor is eliminated by estimating the rotor's angular speed, and the MRAS approach offers a sturdy alternative for this purpose. The presented approach provides a robust alternative, where the adaptation mechanism is facilitated by the implementation of a Deadbeat regulator. This mechanism allows for an improved response and superior control in motor operations, thus making sensor-based systems less necessary. In order to ascertain the efficiency of the proposed method, a comprehensive simulation test was conducted using MATLAB/Simulink.

Keywords: sensorless speed control; induction motors; Model Reference Adaptive System; Deadbeat regulator; field-oriented control

Citation: Hamdi, W.; Hammoudi, M.Y.; Betka, A. Sensorless Speed Control of Induction Motor Using Model Reference Adaptive System and Deadbeat Regulator. *Eng. Proc.* **2023**, *56*, 16. https://doi.org/10.3390/ASEC2023-15240

Academic Editor: Andrea Ballo

Published: 26 October 2023

1. Introduction

Induction motors have long been the workhorse of the industrial world, revered for their robustness, reliability, and remarkable versatility [1]. Their wide range of applications, extending from powering simple domestic appliances to driving large-scale industrial machinery, is a testament to their indispensability [2]. Despite their simplicity in construction, the performance of induction motors significantly depends on the ability to effectively regulate and control their speed. Thus, their control has been a focus of rigorous research, leading to numerous methods and techniques with varying levels of complexity and effectiveness [3–6].

Over the years, several control techniques for induction motors have been developed, each with its own unique characteristics. Scalar control, or Volts/Hertz control, provides a simple approach, but it lacks precision in dynamic performance [7]. On the other hand, Field-Oriented Control (FOC), also known as vector control, allows for independent control of the motor's speed and torque, significantly improving dynamic response and precision [8]. Direct Torque Control (DTC) is yet another method that directly controls the motor's torque and flux, providing excellent dynamic response, but with a higher torque ripple and variable switching frequency [9]. These three control techniques form the cornerstone of induction motor control, each offering different levels of simplicity, performance, and precision. Hence, finding an optimal control technique that balances precision, complexity, and cost has become a quest of paramount importance.

A significant factor contributing to the cost and complexity of the control process is the need for accurate speed estimation. Often, a separate sensor, such as an encoder or tachometer, is used to monitor the speed of the motor. However, these sensors not

only add to the cost but also complicate the system by introducing additional components that require maintenance and are prone to failure. Consequently, research is veering towards sensorless control techniques that can effectively estimate motor speed without needing dedicated speed sensors, thereby reducing the cost and complexity of the control process [10–12].

In this paper, we propose a novel approach to sensorless speed control of induction motors using the Model Reference Adaptive System (MRAS) method, leveraging the Deadbeat regulator in the adaptation mechanism. The Deadbeat regulator, known for its capacity to achieve system response in the minimum possible time, will be instrumental in providing fast and accurate speed estimation. By employing the MRAS method with the Deadbeat regulator, we aim to create a robust, cost-effective, and precise control mechanism, thereby contributing a significant advancement in the field of induction motor control.

The paper is systematically organized into eight sections: Section 2 presents the mathematical model of the induction motor; Section 3 explores the synthesis of the Deadbeat regulator; Section 4 unpacks the components and functions of the MRAS; Section 5 outlines the design of the Deadbeat regulator for the MRAS adaptation mechanism; Section 6 elucidates the structure of sensorless-based Field-Oriented Control Drive; Section 7 illustrates the simulation results; and finally, Section 8 draws the conclusions from our research. Each section serves as a building block in understanding our proposed sensorless speed control method for induction motors.

2. Mathematical Model of Induction Motor

The mathematical model of an induction motor using the Park transformation method in the stationary reference frame, the $\alpha - \beta$ reference frame, and complex notation by considering that the "α" axis is aligned with the real axis, and the "β" axis is aligned with the imaginary axis, where

$$\bar{X}_{(\alpha,\beta)} = X_\alpha + jX_\beta \tag{1}$$

is given as follows:

$$\overline{V_S}_{(\alpha,\beta)} = R_s\overline{I_S}_{(\alpha,\beta)} + \frac{d\overline{\Psi_S}_{(\alpha,\beta)}}{dt} \tag{2}$$

$$\overline{Vr}_{(\alpha,\beta)} = \mathrm{R_r}\,\overline{I_r}_{(\alpha,\beta)} + \frac{d\overline{\Psi_r}_{(\alpha,\beta)}}{dt} - j\omega_e\overline{\Psi_r}_{(\alpha,\beta)} \tag{3}$$

$$\overline{\Psi s}_{(\alpha,\beta)} = Ls\overline{Is}_{(\alpha,\beta)} + \mathrm{Lm}\,\overline{Ir}_{(\alpha,\beta)} \tag{4}$$

$$\overline{\Psi r}_{(\alpha,\beta)} = Lr\overline{Ir}_{(\alpha,\beta)} + \mathrm{Lm}\,\overline{Is}_{(\alpha,\beta)} \tag{5}$$

where:
X_α and X_β are the α and β component, respectively.
$\overline{Vs}$ and $\overline{Vr}$ are the complex stator and rotor voltages, respectively.
$\overline{\Psi s}$ and $\overline{\Psi r}$ are the complex stator and rotor flux, respectively.
$\overline{Is}$ and $\overline{Ir}$ are the complex stator and rotor currents, respectively.
ω_e is the rotor electrical speed.
Rs and Rr are the stator and rotor resistance, respectively.
Ls, Lr and Lm are the stator, rotor, and mutual inductance, respectively.

3. Deadbeat Regulator Synthesis

The Deadbeat algorithm is designed to guide the output from an arbitrary initial state to a desired final state in the minimum number of sampling times. The design of the Deadbeat algorithm depends on the knowledge of the model of the system to be regulated. This control strategy is a key component in the adaptation mechanism of the Model Reference Adaptive System that will be addressed in the following section.

Figure 1 below represents an example where the input is a step function:

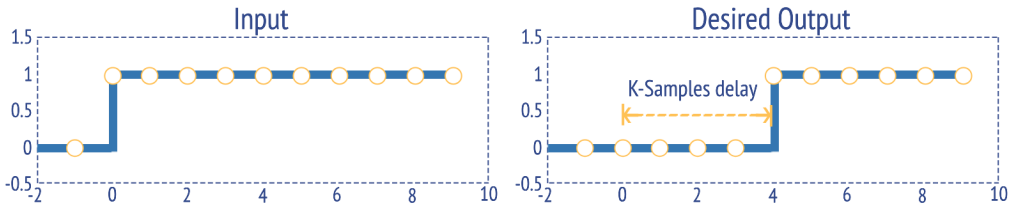

Figure 1. Example of the operation of the Deadbeat regulator.

Using the Z-transform, the closed-loop transfer function of the system that led to this response is:

$$G_{CL}(z) = Z^{-K} \quad where \;\; K \geq 1 \tag{6}$$

The coefficient K corresponds to the number of samples required for the output to reach the desired value. The Z-transform of the Deadbeat regulator is deduced as follows:

$$D(z) = \frac{1}{G_{OL}(z)} \times \frac{G_{CL}(z)}{1 - G_{CL}(z)} = \frac{1}{G_{OL}(z)} \times \frac{Z^{-K}}{1 - Z^{-K}} \tag{7}$$

Using the Deadbeat regulator, all the poles of the closed-loop transfer function are at the origin of the Z plane [13,14]. When the poles of the closed-loop transfer function are located at the origin of the Z plane, it means that the response is as fast as possible. The control loop is represented in Figure 2:

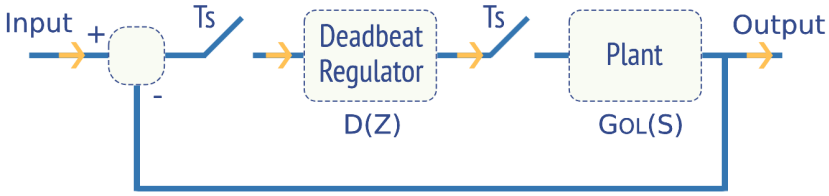

Figure 2. The loop of the Deadbeat regulator.

4. Model Reference Adaptive System

The Model Reference Adaptive System is principally developed to minimize the error between actual and estimated values. In this work, it is employed for determining the rotation speed of the induction motor, utilizing only the measurements of the stator voltage and current. The MRAS approach uses two structures of machine models to estimate the same state variable (Figure 3). The model that does not include the estimated variable, the rotor speed, is referred to as the "Reference model", while the other one as the "Adjustable model" [15]. These models are compared, and any ensuing error is directed towards an "Adaptation mechanism".

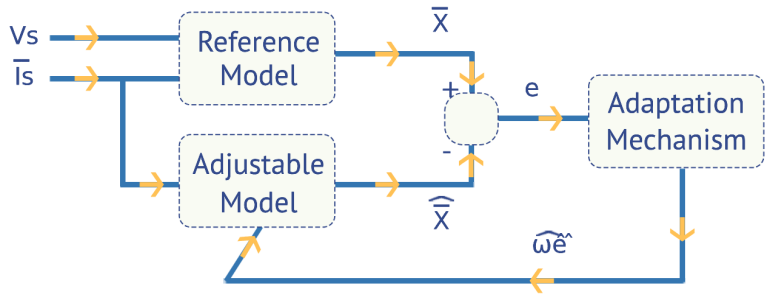

Figure 3. MRAS-based speed estimator scheme.

Within this framework, the state variable to be estimated—which is also the output variable of each model—is the rotor flux. To achieve this, the rotor flux equation derived from the stator equations forms the reference model. Simultaneously, the same variable, deduced from the rotor equations associated with the electrical speed, makes up the adjustable model.

4.1. Reference Model

The equation for the stator voltage (2) should be rewritten in terms of the state to be estimated, which is the rotor flux. From Equation (5), we obtain:

$$\overline{Ir}_{(\alpha,\beta)} = \frac{\overline{\Psi r}_{(\alpha,\beta)} - Lm \times \overline{Is}_{(\alpha,\beta)}}{Lr} \tag{8}$$

By substituting (8) into the expression of the stator flux (4), the following equation is obtained:

$$\overline{\Psi s}_{(\alpha,\beta)} = \frac{Lm}{Lr} \times \overline{\Psi r}_{(\alpha,\beta)} + Ls \times \sigma \times \overline{Is}_{(\alpha,\beta)} \tag{9}$$

By replacing (9) in (2), we obtain:

$$\dot{\overline{\Psi r}}_{(\alpha,\beta)} = \frac{Lr}{Lm} \times \left(\overline{Vs}_{(\alpha,\beta)} - Rs \times \overline{Is}_{(\alpha,\beta)} + \sigma.L_s.s.\overline{Is}_{(\alpha,\beta)} \right) \tag{10}$$

Equation (10) depicts the gradient of the rotor flux, and since it does not depend on the rotational speed, this equation is chosen as the reference model.

4.2. Adjustable Model

By substituting (8) into the expression of the rotor voltage (3), the following equation is obtained:

$$\dot{\overline{\Psi r}}_{(\alpha,\beta)} = \left(-\frac{1}{Tr} + j.\omega_e \right) \times \overline{\Psi r}_{(\alpha,\beta)} + \frac{Lm}{Tr} \times \overline{Is}_{(\alpha,\beta)} \tag{11}$$

Equation (11) depends on the rotor speed, which is why it is considered as the adjustable model, and the rotor flux obtained from it is the estimated flux. Therefore, Equation (11) becomes:

$$\dot{\widehat{\overline{\Psi r}}}_{(\alpha,\beta)} = \left(-\frac{1}{Tr} + j.\widehat{\omega_e} \right) \times \widehat{\overline{\Psi r}}_{(\alpha,\beta)} + \frac{Lm}{Tr} \times \overline{Is}_{(\alpha,\beta)} \tag{12}$$

4.3. Adaptation Mechanism

The role of the adaptation mechanism is to adjust the error between the reference model and the adjustable model to ensure both the stability of the estimation system and that the estimated value converges towards the reference value.

The error between the value estimated by the adjustable model and the supposedly exact value of the reference model will be noted as:

$$\bar{e} = e_\alpha + j e_\beta = \overline{\Psi r}_{(\alpha,\beta)} - \widehat{\overline{\Psi r}}_{(\alpha,\beta)} \tag{13}$$

In the case where $\widehat{\omega_e} = \omega_e$, Equation (11) can be used as the reference model in the analysis of the adaptation mechanism because it provides the exact value of the flux [16].

Therefore, the dynamic error between the two models (11) and (12) is:

$$\frac{d}{dt}\begin{bmatrix} e_\alpha \\ e_\beta \end{bmatrix} = \begin{bmatrix} -\frac{1}{Tr} & \omega_e \\ \omega_e & -\frac{1}{Tr} \end{bmatrix} \times \begin{bmatrix} e_\alpha \\ e_\beta \end{bmatrix} - \begin{bmatrix} \widehat{\Psi r}_\beta \\ -\widehat{\Psi r}_\alpha \end{bmatrix} \times (\omega_e - \widehat{\omega_e}) \tag{14}$$

This model is equivalent to:

$$\frac{d}{dt}[e] = [A] \times [e] - [W] \tag{15}$$

Several methods are used to study the stability of this error dynamic, among which the POPOV inequality that is usually used in the literature, which leads us to the following MRAS structure (Figure 4):

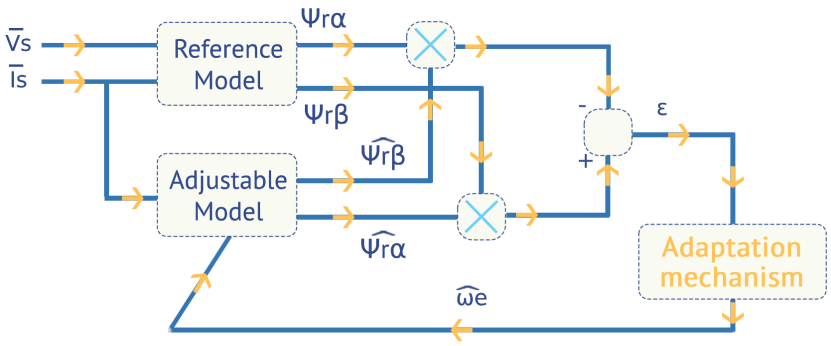

Figure 4. Block Diagram of the MRAS.

Where ε is the error intended for the corrector, which is calculated according to the cross product as follows:

$$\varepsilon = \Psi r_\beta \times \widehat{\Psi r}_\alpha - \Psi r_\alpha \times \widehat{\Psi r}_\beta \tag{16}$$

In the following section, the identification of the adaptation mechanism is presented based on the Deadbeat regulator instead of the "PI" usually used in the literature.

5. Adaptation Mechanism Based on Deadbeat Regulator

Generally, the variables $\hat{\omega}_e$ and ω_e are not constant but change over time, and each one can be considered as an input to a system that is defined by Equation (11). To explore the dynamic behavior of the MRAS, the equations need to be linearized for small deviations around a specific steady-state solution. It is beneficial to initially convert the equations to reference frame d-q that rotates in sync with the stator current vector to benefit from its properties compared to the $\alpha - \beta$ reference frame. By doing so, the resulting equations would be as follows [17]:

$$\frac{d}{dt}\begin{bmatrix} \Delta\Psi r_d \\ \Delta\Psi r_q \end{bmatrix} = \begin{bmatrix} -\frac{1}{Tr} & \omega_{s0} - \omega_{e0} \\ \omega_{e0} - \omega_{s0} & -\frac{1}{Tr} \end{bmatrix}\begin{bmatrix} \Delta\Psi r_d \\ \Delta\Psi r_q \end{bmatrix} + \frac{Lm}{Tr}\begin{bmatrix} \Delta is_d \\ \Delta is_q \end{bmatrix} + \begin{bmatrix} -\Psi r_{q0} \\ \Psi r_{d0} \end{bmatrix}\Delta\omega_e \tag{17}$$

$$\frac{d}{dt}\begin{bmatrix} \Delta\widehat{\Psi r}_d \\ \Delta\widehat{\Psi r}_q \end{bmatrix} = \begin{bmatrix} -\frac{1}{Tr} & \omega_{s0} - \widehat{\omega_{e0}} \\ \widehat{\omega_{e0}} - \omega_{s0} & -\frac{1}{Tr} \end{bmatrix}\begin{bmatrix} \Delta\widehat{\Psi r}_d \\ \Delta\widehat{\Psi r}_q \end{bmatrix} + \frac{Lm}{Tr}\begin{bmatrix} \Delta is_d \\ \Delta is_q \end{bmatrix} + \begin{bmatrix} -\widehat{\Psi r}_{q0} \\ \widehat{\Psi r}_{d0} \end{bmatrix}\Delta\hat{\omega}_e \tag{18}$$

The error function ε (16) takes the form of an inner product vector, which remains independent of the reference frame in which the vectors are expressed. Therefore, it can be represented by the following linearized expression:

$$\Delta\varepsilon = \left(\Psi r_{q0} \times \Delta\widehat{\Psi r}_d - \Psi r_{d0} \times \Delta\widehat{\Psi r}_q\right) - \left(\widehat{\Psi r}_{q0} \times \Delta\Psi r_d - \widehat{\Psi r_{d0}} \times \Delta\Psi r_q\right) \tag{19}$$

From these equations, we can derive the transfer function linking $\Delta\omega_e$ to $\Delta\varepsilon$ as follows:

$$G(S) = \left.\frac{\Delta\varepsilon}{\Delta\omega_e}\right|_{\Delta\hat{\omega}_e=0} = \left.\frac{\Delta\varepsilon}{-\Delta\hat{\omega}_e}\right|_{\Delta\omega_e=0} = \frac{\left(s + \frac{1}{T_r}\right) \times |\Psi_{r0}|^2}{\left(s + \frac{1}{T_r}\right)^2 + (\omega_{s0} - \omega_{e0})^2} \tag{20}$$

where $|\Psi_{r0}|^2 = \left(\Psi r_{d0}{}^2 + \Psi r_{q0}{}^2\right)$ is the flux modulus, and it is assumed that $\Psi r_{q0} = \widehat{\Psi r}_{q0}$ and $\Psi r_{d0} = \widehat{\Psi r}_{d0}$.

The slip pulsation $\omega_{g0} = \omega_{s0} - \omega_{e0}$ in Equation (20) will be smaller as the slip g approaches zero. This corresponds to a "no-load" operation, when the torque moment

demanded by the load is relatively weak compared to the nominal torque moment, which can be a problem at low speed. By neglecting the slip pulsation, the transfer function (20) becomes:

$$G(S) = \frac{\Delta\varepsilon}{\Delta\omega_e}\Big|_{\Delta\widehat{\omega}_e=0} = \frac{|\Psi_{r0}|^2}{s+\frac{1}{T_r}} = \frac{T}{s+R} \tag{21}$$

where $T = |\Psi_{r0}|^2$ and $R = \frac{1}{T_r}$.

In order to obtain the Deadbeat regulator, the Z-transform of Equation (21) must be deduced:

$$G(Z) = \frac{T}{R} \times \frac{1-e^{-R\times Te}}{(Z-e^{-R\times Te})} \tag{22}$$

By substituting Equation (22) into Equation (7), we obtain:

$$D(z) = \frac{R\times\left(Z-e^{-R\times Te}\right)}{T\times\left(1-e^{-R\times Te}\right)} \times \frac{1}{Z-1} \tag{23}$$

Figure 5 illustrates the structure of the speed regulator:

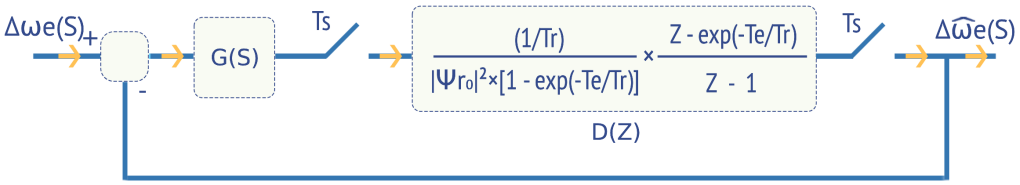

Figure 5. Deadbeat Regulator for Speed Estimation.

6. Structure of Sensorless-Based Field-Oriented Control Drive

Figure 6 presents the diagram of the proposed indirect field-oriented control based on the MRAS speed identification and tailored for the induction motor drive. This architecture employs dual-nested loops in both the d and q axes. The associated controllers are used to formulate the reference stator voltages Vds^* and Vqs^*.

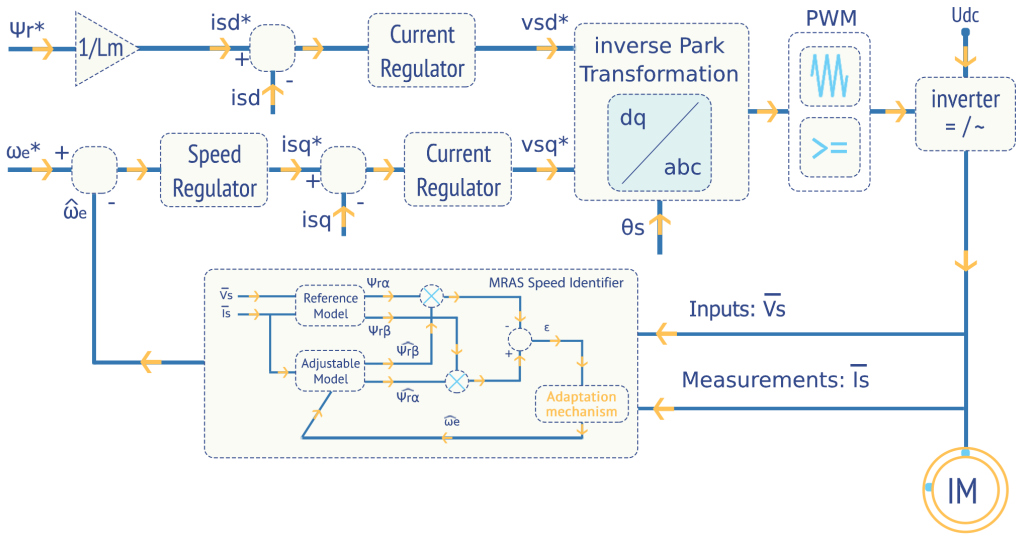

Figure 6. The block diagram of sensorless field-oriented control.

7. Simulation Results

To evaluate the effectiveness of the proposed regulator and compare it with the conventional "PI" regulator, a simulation test was conducted. The test took into account a speed profile that began at $\omega = 100$ (rad/s), then moved to $\omega = -100$ (rad/s) at $t = 2$ (s).

The rotor reference flux was set to 0.8 (Wb) and the Load torque was applied at $T_L = 20$ (Nm) at $t = 0.5$ (s). The parameters of the PI regulator of the adaptation mechanism were $K_i = 31062$ and $K_p = 126.35$. In order to test the stability of the estimation error and make sure that it converges to zero, we added different initial conditions between the speed of the real system and the adjustable model.

The parameters of the induction motor are given in Table 1 below [18]:

Table 1. Induction Motor Parameters.

Parameters	Values
Moment of inertia	$Jm = 0.049$ [Kg.m^2]
Stator resistance	$R_s = 6.06$ [Ω]
Rotor resistance	$R_r = 4.2$ [Ω]
Rated flux	$\Psi n = 0.946$ [Wb]
Mutual stator-rotor inductance	$L_m = 0.44$ [H]
Stator inductance	$L_s = 462$ [mH]
Rotor inductance	$L_r = 462$ [mH]
Pole pairs	$p = 2$
Friction coefficient	$f = 0.0032$ [Nm/rad/s]

Figures 7 and 8 are indeed insightful in evaluating the comparative performance of the proposed "Deadbeat" regulator against the traditional "PI" method. In Figure 7, it is apparent that the proposed regulator demonstrates superior tracking of the real state over the conventional approach. This could be indicative of a more accurate and rapid response mechanism inherent in the proposed regulator, making it potentially more effective in real-world applications where time-sensitive regulation might be crucial. Figure 8 further reinforces the effectiveness of the proposed regulator. It clearly illustrates a faster convergence of the estimation error to zero, with noticeably less overshoot than that exhibited by the conventional "PI".

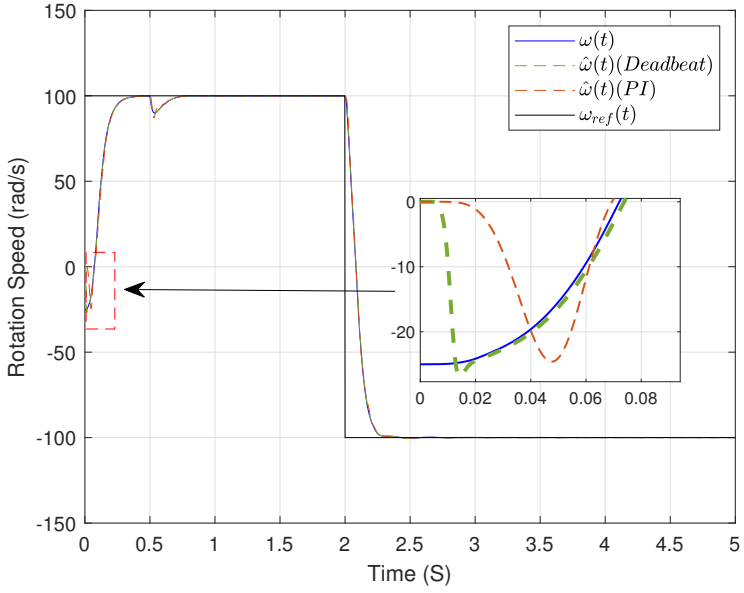

Figure 7. Rotor angular speed curve.

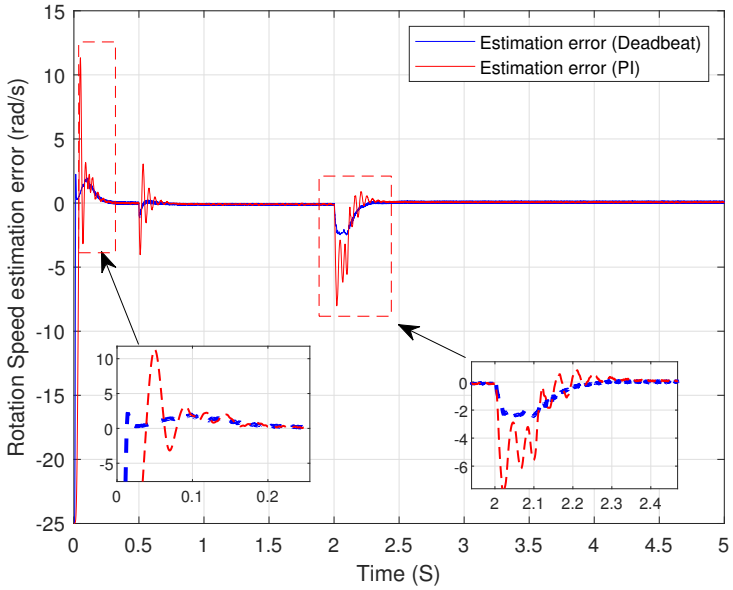

Figure 8. Rotor angular speed estimation error.

8. Conclusions

In conclusion, this paper has successfully presented an innovative approach towards reducing control process costs by eliminating the need for speed sensors in the control of induction motors. It showcases the effectiveness of sensorless speed control using a Model Reference Adaptive System, notably using the 'Deadbeat' regulator as an adaptive mechanism. When compared to the conventional 'PI' regulator, the 'Deadbeat' regulator exhibits superior performance, demonstrates improved response time, and reduced overshoot during the estimation process.

Despite these significant advancements, certain limitations of the 'Deadbeat' regulator have been identified, specifically its dependence on accurate mathematical system models and its sensitivity to parameter variations. These challenges delineate potential directions for future research, underscoring the pursuit of even more robust and flexible control strategies for induction motors.

Author Contributions: Conceptualization, W.H. and A.B.; methodology, W.H.; software, W.H.; validation, W.H.; investigation, W.H. and A.B.; writing—original draft preparation, W.H., A.B. and M.Y.H.; writing—review and editing, W.H., A.B. and M.Y.H.; visualization, W.H., A.B. and M.Y.H.; supervision, A.B.; project administration, A.B. All authors have read and agreed to the published version of the manuscript.

Funding: This research received no external funding

Institutional Review Board Statement: Not applicable

Informed Consent Statement: Not applicable

Data Availability Statement: Data sharing not applicable

Conflicts of Interest: The authors declare no conflict of interest

References

1. Lee, K.; Han, Y. Reactive-power-based robust MTPA control for v/f scalar-controlled induction motor drives. *IEEE Trans. Ind. Electron.* **2021**, *69*, 169–178. [CrossRef]
2. Kumar, S.; Mukherjee, D.; Guchhait, P.K.; Banerjee, R.; Srivastava, A.K.; Vishwakarma, D.N.; Saket, R.K. A comprehensive review of condition based prognostic maintenance (CBPM) for induction motor. *IEEE Access* **2019**, *7*, 90690–90704. [CrossRef]
3. Zhang, Y.; Yin, Z.; Li, W.; Liu, J.; Zhang, Y. Adaptive sliding-mode-based speed control in finite control set model predictive torque control for induction motors. *IEEE Trans. Power Electron.* **2020**, *36*, 8076–8087. [CrossRef]

4. Arshad, M.H.; Abido, M.A.; Salem, A.; Elsayed, A.H. Weighting factors optimization of model predictive torque control of induction motor using NSGA-II with TOPSIS decision making. *IEEE Access* **2019**, *7*, 177595–177606. [CrossRef]
5. Mahfoud, M.E.; Bossoufi, B.; Ouanjli, N.E.; Said, M.; Taoussi, M. Improved Direct Torque Control of Doubly Fed Induction Motor Using Space Vector Modulation. *Int. J. Intell. Eng. Syst.* **2021**, *14*, 177–188. [CrossRef]
6. El Ouanjli, N.; Motahhir, S.; Derouich, A.; El Ghzizal, A.; Chebabhi, A.; Taoussi, M. Improved DTC strategy of doubly fed induction motor using fuzzy logic controller. *Energy Rep.* **2019**, *5*, 271–279. [CrossRef]
7. dos Santos, T.H.; Goedtel, A.; da Silva, S.A.O.; Suetake, M. Scalar control of an induction motor using a neural sensorless technique. *Electr. Power Syst. Res.* **2014**, *108*, 322–330. [CrossRef]
8. Cai, W.; Wu, X.; Zhou, M.; Liang, Y.; Wang, Y. Review and development of electric motor systems and electric powertrains for new energy vehicles. *Automot. Innov.* **2021**, *4*, 3–22. [CrossRef]
9. El Ouanjli, N.; Derouich, A.; El Ghzizal, A.; Motahhir, S.; Chebabhi, A.; El Mourabit, Y.; Taoussi, M. Modern improvement techniques of direct torque control for induction motor drives-a review. *Prot. Control. Mod. Power Syst.* **2019**, *4*, 11. [CrossRef]
10. Korzonek, M.; Tarchala, G.; Orlowska-Kowalska, T. A review on MRAS-type speed estimators for reliable and efficient induction motor drives. *Isa Trans.* **2019**, *93*, 1–13. [CrossRef] [PubMed]
11. Van Pham, T.; Vo Tien, D.; Leonowicz, Z.; Jasinski, M.; Sikorski, T.; Chakrabarti, P. Online rotor and stator resistance estimation based on artificial neural network applied in sensorless induction motor drive. *Energies* **2020**, *13*, 4946. [CrossRef]
12. Zuo, Y.; Ge, X.; Zheng, Y.; Chen, Y.; Wang, H.; Woldegiorgis, A.T. An adaptive active disturbance rejection control strategy for speed-sensorless induction motor drives. *IEEE Trans. Transp. Electrif.* **2022**, *8*, 3336–3348. [CrossRef]
13. Xu, C.; Han, Z.; Lu, S. Deadbeat predictive current control for permanent magnet synchronous machines with closed-form error compensation. *IEEE Trans. Power Electron.* **2019**, *35*, 5018–5030. [CrossRef]
14. Pfeifle, O.; Fichter, W. Time-Optimal Incremental Nonlinear Dynamic Inversion through Deadbeat Control. In Proceedings of the AIAA Scitech 2022 Forum, San Diego, CA, USA, 3–7 January 2022; p. 1596.
15. Bednarz, S.A.; Dybkowski, M. Estimation of the induction motor stator and rotor resistance using active and reactive power based model reference adaptive system estimator. *Appl. Sci.* **2019**, *9*, 5145. [CrossRef]
16. Chaigne, C.; Etien, E.; Cauët, S.; Rambault, L. *Commande Vectorielle Sans Capteur des Machines Asynchrones*; Hermes-Lavoisier: Paris, France, 2005.
17. Schauder, C. Adaptive speed identification for vector control of induction motors without rotational transducers. In Proceedings of the Conference Record of the IEEE Industry Applications Society Annual Meeting, San Diego, CA, USA, 1–5 October 1989; pp. 493–499
18. Abdelati, R.; Mimouni, M.F. Minimum-energy consumption of an induction motor operating in dynamic regime. *J. Electr. Eng.* **2010**, *10*, 11.